Geotechnical Aspects of Underground Construction in Soft Ground – Viggiani (ed)
© 2012 Taylor & Francis Group, London, ISBN 978-0-415-68367-8

The horizontal response of framed buildings on individual footings to excavation-induced movements

K.H. Goh
Land Transport Authority, Singapore (formerly from University of Cambridge)

R.J. Mair
University of Cambridge, UK

ABSTRACT: Deep excavations and tunnelling can cause ground movements that affect buildings within their influence zone. The current approach for building damage assessment is based on tensile strains estimated from the deflection ratio and the horizontal strains at the building foundation. This paper examines the significance of horizontal strains in buildings on individual footings. The first part of the paper presents a case study of a framed building in Singapore which was subjected to the effects of bored tunnelling, where significant horizontal strains were observed. The second part of the paper suggests a method to relate the horizontal strains induced in a building to the stiffness of the frame structure. Using a combination of simplified structural analysis and finite element models, design guidance is proposed to estimate excavation-induced horizontal strains in frame buildings on individual footings.

1 INTRODUCTION

Activities associated with deep excavations and tunnelling can cause ground movements that affect buildings within their zone of influence. The current approach for building damage assessment is based on the maximum tensile strains estimated from the deflection ratio and the horizontal strains at the foundation level (Mair et al, 1996). Recent studies have shown that the deflection ratio and the horizontal strains induced in the building can be reduced significantly if the building is on continuous footings (Mair, 2003). In contrast, the response of buildings on individual footings is not as well investigated.

Goh & Mair (2010) presented a case history on the settlement response of two reinforced concrete framed buildings above the bored tunnelling works for a section of the Singapore Circle Line, and showed that the inherent stiffness of framed buildings can influence their settlement response to tunnelling- and excavation-induced movements. To quantify this influence, a column stiffening factor was suggested to relate the bending stiffness of framed buildings to that of simple beams so that the deflection ratio of the building can be estimated from plots of building modification factors against relative bending stiffness (similar to the design curves proposed by Potts & Addenbrooke, 1997).

In terms of horizontal strains, Elshafie (2008) conducted centrifuge experiments of buildings behind a cantilever excavation in sand. He observed that a building modelled using a block sitting directly on the ground has horizontal strains which are low compared to the greenfield condition and depend on the stiffness of the building block. However, when the building is modelled using a block supported on two footings at each end, significant horizontal distortion to the building was observed especially at the block-footing interface.

In this paper, the behaviour of framed buildings on individual footings in terms of horizontal strains induced by tunnelling and deep excavations is examined. The first part of the paper presents a case study of two rows of shop houses that were subjected to the effects of bored tunnelling—this is the same site in Goh & Mair (2010) except that this paper focuses on the horizontal strain response in the framed buildings whilst the previous paper focused only on the settlement behaviour. For completeness, a summary of the settlement behaviour is also given in this paper.

In the second part of the paper, an attempt to quantify the influence of building stiffness is made for frame structures on individual footings. Using structural analysis, a method to estimate the horizontal stiffness of framed buildings is suggested. The finite element method was then used to study the response of frame structures adjacent to deep excavations, and to suggest design guidance for rigidly-connected frame buildings on individual footings.

2 CASE STUDY OF THE PASIR PANJANG SHOP HOUSES

2.1 *Site description*

A section of the tunnels in Contract 856 of the Singapore Circle Line was constructed using twin bored tunnelling drives, below two blocks of shop houses along the Pasir Panjang (PPJ) Road. These units were labelled as A29 and A32 during construction (Fig. 1). The bored tunnelling was done using earth-pressure balance shield machines, and was described by Venkta et al (2008). The first (inner) tunnel was constructed away from the shop houses, whilst the second (outer) tunnel was constructed directly below the shop houses. The depths to the tunnel axis ranged from 16 m to 19 m at this location.

Constructed together in the 1960s, the shop houses are two-storey, reinforced-concrete framed buildings. The columns are supported on shallow foundations of individual footings supported by timber bakau piles, whose lengths were estimated to be from 6 m to 9 m. At the ground floor, there are tie-beams connecting the main columns of the frame, but not all columns are connected in both directions. In particular, the columns along the five-foot-way—a common corridor which is about five foot wide—are unconnected at the ground floor level. The ground floor slab is of a non-suspended type. At the first floor, the beams connect all the columns together in a grid (including the columns above the five-foot-way) as they transfer the loads from the first floor slabs down to the foundation. The first floor slab is about 100 mm thick. As the roof is pitched and tiled, the roof beams are lightly loaded and mainly used for tying the main columns together. The building façade and internal walls are mostly formed using brick in-fills, whilst the walls at the rear of the shop houses are supported on strip footings and unconnected to the frame structure.

The geology at this location comprises the fluvial and marine deposits of the Kallang Formation over-lying the soils and rocks of the Jurong Formation whose members have varied sedimentary origins but commonly exhibiting evidence of metamorphism. Along this section of the bored tunnels, the ground typically consists of about 3 m of Fill underlain by a 9 m–14 m thick layer of Kallang Formation (of estua-rine, fluvial sand, fluvial clay and marine clay), and overlying the various weathering grades of Jurong Formation rocks. Locally, there is a thick layer of fluvial sand under shop house A32 and a substantial layer of compressible clays below the shop house A29. The bored tunnels were constructed in a mixed face condition of the Kallang Formation and the Ju-rong Formation, with a –2.5% gradient dip in the vertical alignment westwards along the tunnel drive. Figure 2 shows the cross sections of the shop houses and the soil profiles.

A detailed instrumentation programme was implemented during the bored tunnelling works. This included ground and building settlement markers, and tape extensometers measurements between columns. Whilst the settlement response

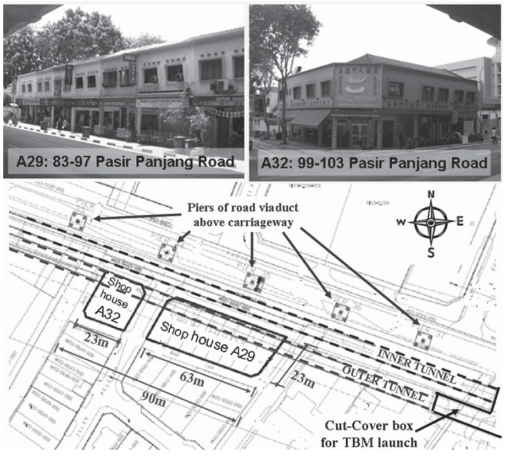

Figure 1. Location of the PPJ shop houses.

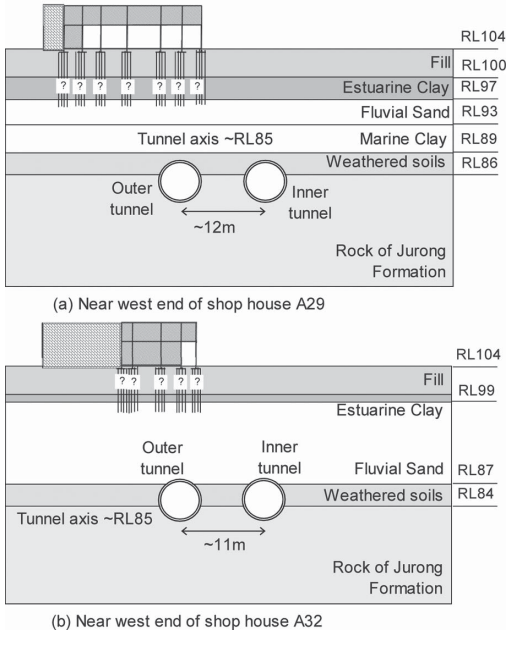

Figure 2. Cross-sections of the shop houses and soil profiles.

of the PPJ shop houses was described in Goh & Mair (2010), the monitoring results from the tapeextensometer are presented in this paper. Figure 3 shows the layout of the settlement monitoring and Figure 4 shows the tape extensometer measurements in the shop houses.

2.2 *Settlement behaviour*

As presented in Goh & Mair (2010), the settlement of the shop houses was monitored in four arrays. At the eastern-most section of shop house A29, there is a ground settlement array E14 (Fig. 3a) alongside to the building settlement array A29east (Fig. 3b). The ground and building settlement markers were observed to be settling several months after the passage of the first tunnel, and this makes it difficult to differentiate settlements due to the second tunnel drive alone. As such, the ground and building settlement troughs transverse to the direction of tunnel drive, were presented for the first tunnel drive and for both tunnels at the end of the second tunnel drive (see Fig. 5). At this location, the ground surface is settling in a hogging deformation for both tunnel drives. Furthermore, the hogging deformation of the building is very similar to the ground settlement—the building is deflecting very flexibly in this location.

That was the only location where ground settlement markers were monitored alongside building settlement markers. Elsewhere, a greenfield surface settlement trough can be assumed by using a theoretical Gaussian curve and considering the effects of the two tunnel drives separately. This is possible because the building settlement markers at these locations showed that the settlements due to the first tunnel drive had stabilised before the second tunnel drive started. The Gaussian settlement function is given by:

$$S_v = S_{max} e^{(-x^2/2i^2)} \quad (1)$$

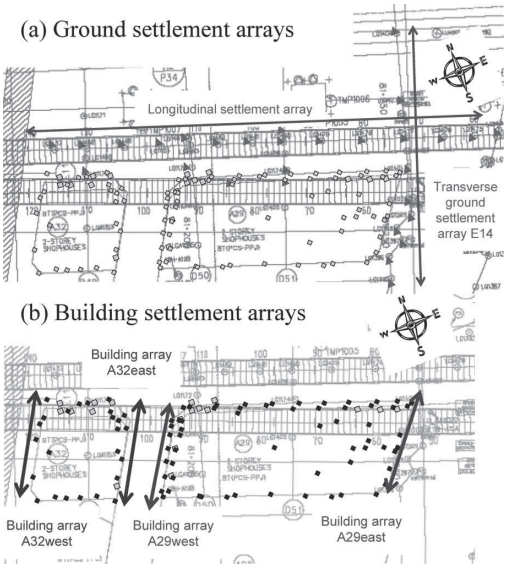

Figure 3. Layout of building and ground settlement markers.

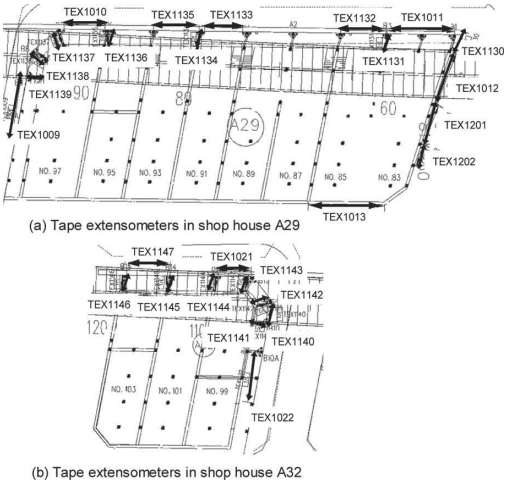

Figure 4. Layout of tape extensometer monitoring.

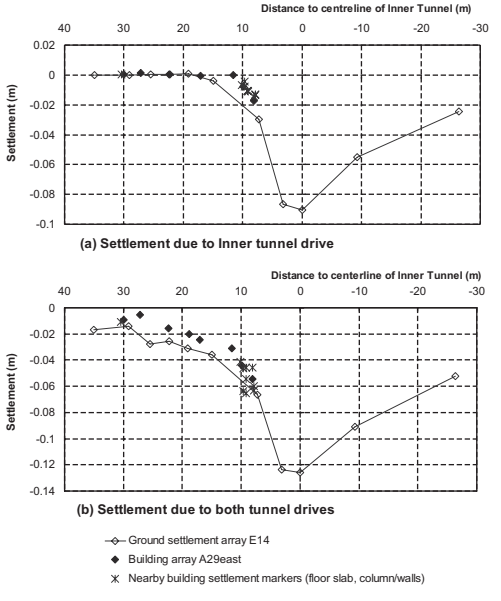

Figure 5. Ground and building settlement at east end of shop house A29.

where S_v is the ground surface settlement with a maximum value $S_{max} = V_L * \pi D^2/4/\sqrt{2\pi} * i$, V_L being the volume loss encountered during tunnelling, D is the tunnel diameter, and the width of the settlement trough, $i = K*z_0$ where K is a trough width parameter and z_0 is the depth to tunnel axis. The trough widths and volume losses can be varied to obtain various greenfield settlement curves.

Figure 6 shows the building settlement at the west end of shop house A29, and a particular greenfield settlement curve assumed using the Gaussian function in each tunnel drive. It was found that a narrow trough width for the Gaussian settlement curve provided a good match to the building settlement behaviour during the first (inner) tunnel drive. This could be due to the fluvial sand layer settling with a narrower trough, and also due to the effect of the bakau pile foundation causing the building to settle with the narrower subsurface settlement trough corresponding to a depth nearer to the pile toe level.

Nevertheless, using the same trough width parameter for the second tunnel drive, the building would be in the sagging deformation region directly above the tunnel and in the hogging deformation region further away from the tunnel. As seen in Figure 6(b), the settlement response of the building is semi-rigid during the second tunnel drive, compared to the greenfield settlement trough. This is in contrast to the flexible behaviour when the building is purely in the hogging deformation mode during the first tunnel drive.

Figure 7 shows the building settlement at both the east end and west end of shop house A32, and a specific greenfield settlement curve using the Gaussian function for each tunnel drive. The behaviour of shop house A32 is similar to that

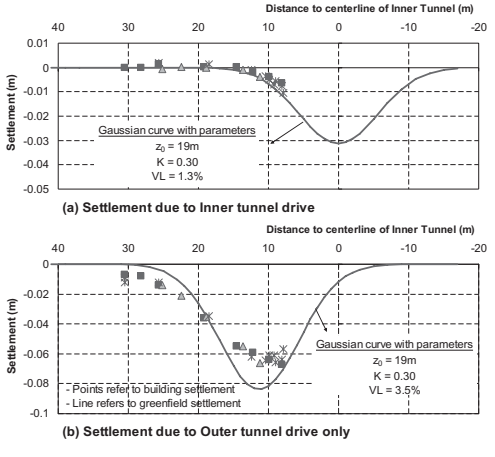

Figure 6. Greenfield and building settlement at west end of shop house A29.

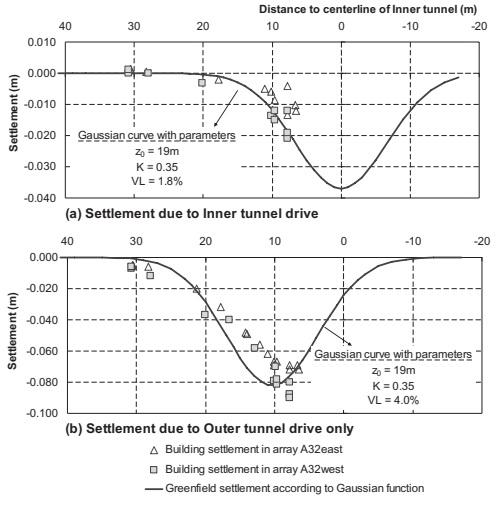

Figure 7. Greenfield and building settlement at both east end and west end of shop house A32.

of shop house A29. When the building is in a purely hogging deformation mode during the first (inner) tunnel drive, the building is very flexible and its settlement behaviour is similar to that of the greenfield. During the second (outer) tunnel drive, the building response is semi-rigid with a sagging deformation mode directly above the tunnel changing to a hogging deformation mode away from the tunnel. Venkta et al (2008) reported that the total building settlement of shop house A32 was up to 100 mm. Although cracks were found on the brick walls and column-brickwall interface, these were non-structural and did not affect the structural integrity of the building. Furthermore, Liew et al (2008) reported that the crack widths generally ranged from 0.3 mm to 1.5 mm, except for an isolated location registering 9.8 mm at an end wall. The crack widths are low as compared to the building settlements.

Using the PPJ shop houses, Goh & Mair (2010) illustrated that the inherent stiffness of framed buildings can influence their settlement response to tunnelling-induced movements. The horizontal response of the PPJ shop houses to tunnelling-induced movements will now be presented.

2.3 *Transverse horizontal strains*

Due to the orientation of the framed building with respect to the tunnelling drive, it is possible to categorise the tape extensometer measurements into those that are transverse to the tunnelling drive and those that are longitudinal. Moreover, the horizontal strains inferred from the tape extensometer measurements were low during the first tunnel

drive, and this is due to the inner tunnel being further away from the building. These became significant during the second tunnel drive when the outer tunnel is directly below the shop houses. As such, only the horizontal strains for the second tunnel drive will be presented.

Figure 8 plots the inferred horizontal strains that are transverse to the tunnelling drive in shop house A29, whilst Figure 9 plots the transverse horizontal strains in shop house A32. Some observations can be made by reviewing the character of the horizontal strains. Firstly, the horizontal strains are mostly compressive. This is due to the tape extensometer measurements made within the sagging trough of the settlement curve where the greenfield horizontal strains are compressive. The tape extensometer measurements showing tensile horizontal strains were further away from the tunnel centreline, and coinciding with the hogging zone of the surface settlement curve. Secondly, the highest horizontal strains occur between columns that are unconnected at the ground floor level and these are mostly along the five-foot-way area. The horizontal strains were as much as 0.24% in compression. This is in contrast to previous case histories of buildings on continuous footings where the horizontal strains in the building were low. Thirdly, for columns that are connected by ground beams, the horizontal strains are much lower (less than 0.04%).

Moreover, it was noted that some of the transverse horizontal strains were initially tensile in

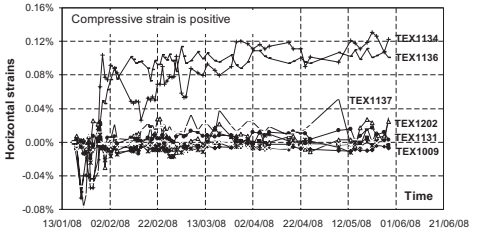

Figure 8. Development of transverse horizontal strains during second tunnel drive in shop house A29.

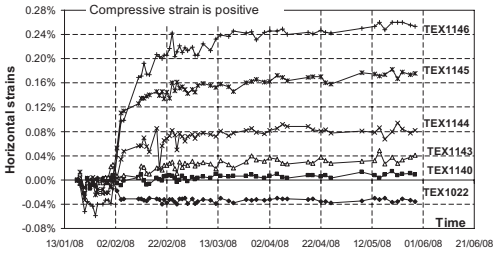

Figure 9. Development of transverse horizontal strains during second tunnel drive in shop house A32.

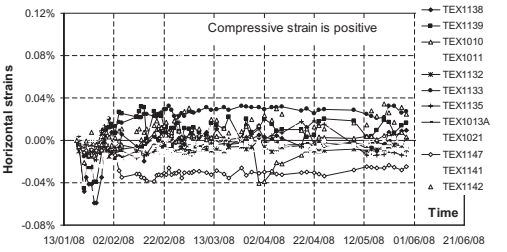

Figure 10. Development of longitudinal horizontal strains in shop house A29 and shop house A32.

nature (up to 0.08%) but changed to compressive at a later stage of the tunnelling. This is probably due to the effects of the advancing tunnelling trough in the longitudinal direction.

2.4 *Longitudinal horizontal strains*

Figure 10 plots the horizontal strains monitored from the tape extensometers that are parallel to the tunnelling direction. Longitudinal horizontal strains (of not more than 0.04%) are lower than the transverse strains, and the occurrence of the maximum strains coincided with the change in the maximum surface settlement monitored in the longitudinal direction. It may be inferred that when the volume loss remains reasonably constant for the tunnelling, the longitudinal horizontal strains would be low.

In general, horizontal strain was observed to be more critical in the transverse direction than the longitudinal direction. Moreover, there is some influence of ground beams on the horizontal strains induced in buildings on individual footings. This is investigated using the finite element method, as described in the following section.

3 NUMERICAL STUDY

3.1 *Finite element analysis*

To investigate the behaviour of framed buildings on individual footings, models of frame structures were simulated adjacent to a multi-propped excavation using the finite element method. Figure 11 shows the parameters of the frame and excavation model used in the study, where the frame columns are unconnected at the footing level. The excavation is 20 m deep and simulated in an undrained condition, whilst the frame is modelled as a weightless structure. The 20 m thick deposit of soft clay overlying a stiff clay stratum is modelled using the Modified Cam Clay, with soil parameters taken from recent soil investigation works in the Singapore Marine Clay.

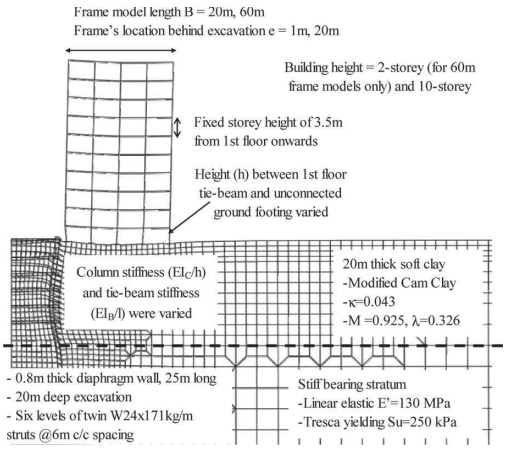

Figure 11. Excavation and soil parameters in model UD_A.

The weightless frame is modelled with various configurations of beam and column stiffness, and the height between the first floor beam and footing was varied. Table 1 shows the variation of frame models for the 20 m and 60 m long buildings, at 1 m and 20 m behind the excavation.

From the finite element models, it was observed that the horizontal displacement of the frame is different from that of the footings. From the first floor upwards, the frame appeared to be moving as a rigid body with very little horizontal strains—this is similar to structures on continuous footings. At the ground floor, there is relative horizontal displacement between the unconnected footings due to the induced movements. As the columns are restrained by the tie-beam at the first floor but much less constrained by the footings at the ground floor, the ground floor columns were showing various tilts in different bays of the frame structure. Due to the differential horizontal movements, substantial horizontal strains occurred between adjacent columns at the ground floor.

Potts & Addenbrooke (1997) proposed the modification factor approach to describe the building response to tunnelling in relation to the greenfield deformation. Specifically in this paper, to describe the average horizontal strains between the footings in terms of the corresponding horizontal strains in the greenfield, the modification factor $M^{\varepsilon h}$ is defined as

$$M^{\varepsilon h} = \frac{\varepsilon_{h,Bldg}}{\varepsilon_{h,GF}} \quad (2)$$

where $\varepsilon_{h,Bldg}$ and $\varepsilon_{h,GF}$ refer to the maximum of the average horizontal strains between adjacent columns in the building and in the greenfield condition respectively.

Table 1. Configuration of frame structure models.

Beam type	1st floor tie-beam type	Column type
100 mm RC slab, with 5 m bay length	100 mm RC slab	150 × 150 mm RC column @5 m 150 mm RC wall
	300 × 300 mm RC beam@5 m	150 × 150 mm RC column @5 m 100 mm RC wall
	250 mm RC slab	150 × 150 mm RC column @5 m 150 mm RC wall
100 mm RC slab, with 10 m bay length	100 mm RC slab	150 × 150 mm RC column @5 m 150 mm RC wall
	250 mm RC slab	150 × 150 mm RC column @5 m
	300 × 300 mm RC beam@5 m	150 × 150 mm RC column @5 m

Furthermore, for buildings on continuous footings, Potts and Addenbrooke proposed a design chart to estimate the horizontal strain modification factor from the relative axial stiffness of the building. Following their definition, the relative axial stiffness (α^*) was calculated for each of the frame models in this study using Equation 3 below:

$$\alpha^* = \frac{EA}{E_S(B/2)} \quad (3)$$

where the axial stiffness of the frame model (EA) is estimated by summing up the axial stiffness of all the individual beams, Es is a representative soil stiffness corresponding to mid-depth of the excavation, and B is the length of the building.

When the horizontal strain modification factors were plotted against the corresponding relative axial stiffness in each frame model, it was found that the modification factors varied from 0 to 1 irrespective of the relative axial stiffness (Fig. 12). Although the axial stiffness for a framed building may be sufficiently high that horizontal strains in the building are small, unconnected footings would still cause significant horizontal strains to the columns at ground floor level. Moreover, there is an important influence of the distance from the footings to the lowest tie beam, as shown in Figure 12. The relative axial stiffness alone does not describe the horizontal response of framed buildings on separate footings.

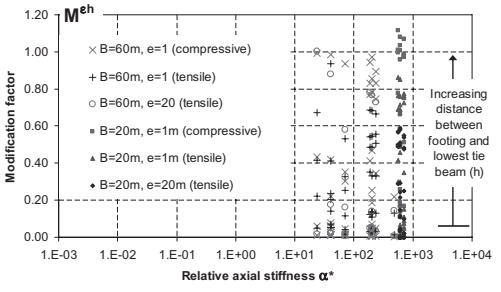

Figure 12. Horizontal strain modification factors for different relative axial stiffness values of frames on separate footings.

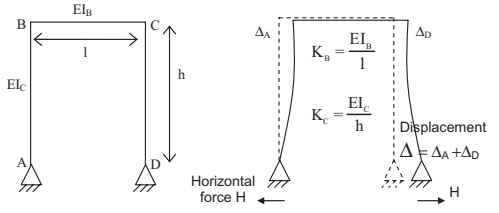

Figure 13. Schematic of simple portal frame.

3.2 *Frame stiffness factor*

A measure of horizontal stiffness for the frame action in the ground floor can be obtained, by determining the force needed to move the support of a structure frame horizontally by a unit displacement. As an approximation, a simple portal frame with a single bay was analysed. As the individual footing is deemed to be unable to offer much moment restraint to the column in the building frame, the simple portal frame was assumed to be pin-supported. A schematic of this portal frame is shown in Figure 13.

The derivation of the stiffness relationship was done by structural analysis using the slope deflection method (Goh, 2010). From the analysis, a frame stiffness factor (α_f) may be defined as

$$\alpha_f = \frac{H}{\Delta} = \frac{3K_B K_C}{h^2(2K_B + 3K_C)} \quad (4)$$

The frame stiffness factor has a dimension of kN/m per metre run, and is dependent on the column height at the ground floor (h), as well as the bending stiffness of the column ($K_C = EI_C/h$) and the first floor tie-beam ($K_B = EI_B/l$).

3.3 *Design guidance for the horizontal strain modification factor*

When the modification factors in Figure 12 are re-plotted against this frame stiffness factor, the results from the different frame-on-individual-footing models appear to fall within a reasonably close band as shown in Figure 14. It is possible to define an upper bound curve with all the modification factors obtained from the various finite element models of the frame structure. This upper bound may be used for design guidance to estimate the horizontal strains in buildings on individual footings or buildings on strip footings that are transverse to the deformation trough.

Using a simple portal frame to derive the frame stiffness factor is clearly a simplification of the actual problem. In reality, frame structures would have bays of different lengths as well as different numbers of upper storeys that would have an influence on the framing action at the ground floor. Furthermore, the portal frame in the structural analysis was pin-supported at its ends. In the actual building, the footing foundation would restrain the rotation of the ground floor columns, and the extent of this restraint—depending on the footing stiffness—would also have an influence on the frame stiffness.

To cope with the simplification, a reasonable upper bound can be derived from amongst all the frame models whose structural elements were varied. For example, additional finite element analyses were completed for frame models above various soil profiles of soft clay and firm soil (Goh, 2010). As shown in Figure 15, the modification factors when plotted against the frame stiffness factor fall within the upper bound curve suggested for design.

Design guidance defined using an upper bound curve will estimate a more flexible response of the horizontal strains for framed buildings on individual footings—this is conservative but acceptable. Nevertheless, it is noted that there is a considerable spread in the modification factors corresponding to each frame stiffness factor. This can be improved by using more rigorous structural frame analysis to define a more refined frame stiffness factor—but which may become complicated to compute.

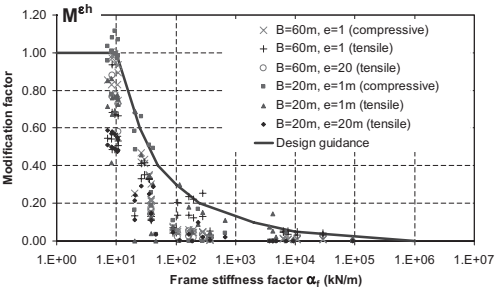

Figure 14. Horizontal strain modification factors for different frame stiffness factors.

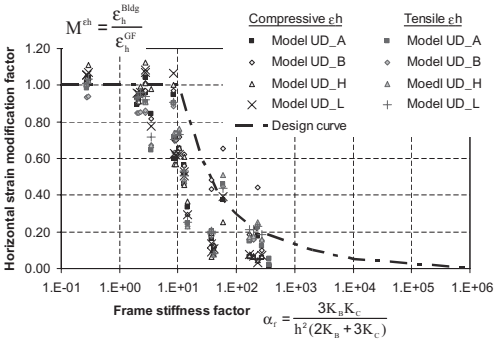

Figure 15. Modification factors for 60 m long, 2-storey frames at 1 m behind excavation in different soil profiles (refer to Goh, 2010 for details of models UD_A, UD_B, UD_H and UD_L).

4 CONCLUSIONS

The horizontal displacement behaviour of buildings on individual footings—including buildings on strip footings that are transverse to the induced ground displacement troughs—is investigated in this paper. While recent research has shown that the horizontal strains for most buildings on continuous footings is reduced significantly, the approach for buildings on individual footings has been to assume the horizontal strains in the greenfield condition.

The case study of the PPJ shop houses has shown the significance of horizontal strains in buildings on individual footings. More importantly, it has illustrated the difference in horizontal strains between columns that are connected by ground beams and columns that are unconnected at ground level but connected at first floor upwards. It was also observed that the transverse horizontal strains in the PPJ shop houses were more significant than the longitudinal horizontal strains.

To study the horizontal displacement behaviour of the rigidly-connected framed building on individual footings, models of frame structures with various configurations behind a multi-propped excavation were analysed using the finite element method. The greatest horizontal strains occur at the ground floor between the unconnected columns, and were observed to be related to the frame stiffness. Using structural analysis of a simple, pin-supported portal frame, a new frame stiffness factor has been defined to describe the horizontal stiffness of a frame structure. By plotting the horizontal strain modification factor against the frame stiffness factor, an upper bound curve has been developed to suggest guidance for estimating the maximum horizontal strains in rigidly-connected frame buildings on individual footings.

ACKNOWLEDGEMENTS

The authors would like to thank Mr. Rama Venkta for providing the information on the bored tunnelling works and the instrumentation monitoring at the PPJ shop houses. The first author would also like to thank the Land Transport Authority of Singapore for sponsoring his research study at the University of Cambridge.

REFERENCES

Elshafie, M.Z.E.B. 2008. *Effect of building stiffness on excavation induced displacements*. Ph.D. thesis, Cambridge University, UK.

Goh, K.H. 2010. Response of ground and buildings to deep excavations and tunnelling. Ph.D thesis, Cambridge University, UK.

Goh, K.H. & Mair, R.J. 2010. Settlement response of framed buildings to movements from tunnelling and deep excavations, *Proc. of World Urban Transit Conference, 20–22 Oct 2010, Singapore*.

Liew, Y.K., Veluvolu, H., Kho, C.M. & Sigl, O. 2008. Risk assessment for earth pressure balancing bored tunnelling under shophouses along Pasir Panjang Road, *Proc. of International Conference on Deep Excavations, 10–12 Nov 2008, Singapore*.

Mair, R.J. 2003. Keynote lecture: Research on tunnelling-induced ground movements and their effects on buildings—lessons from the Jubilee Line Extension. *In F.M. Jardine (ed.), Response of buildings to excavation induced ground movements, Proc. intern. conf., London, 17–18 July 2001*: 3–26. London: CIRIA.

Mair, R.J., Taylor, R.N. & Burland, J.B. 1996. Prediction of ground movements and assessment of risk of building damage due to bored tunnelling, In R.J. Mair and R.N. Taylor (eds.), *Proc. intern. symp. on Geotechnical Aspects of Underground Construction in Soft Ground, London, 15–17 April 1996*: 713–718. Rotterdam: Balkema.

Potts, D.M. & Addenbrooke, T.I. 1997. A structures influence on tunnelling-induced ground movements. *Proc. Institution of the Civil Engineers, Geotechnical Engineering* 125(2): 109–125.

Venkta, R., Hoblyn, S., Mahatma, S. & Lim, H.C. 2008. EPB tunnelling under 2-storey shophouses in mixed face conditions, *Proc. of International Conference on Deep Excavations, 10–12 Nov 2008, Singapore*.